

# Self-Organized Evasive Fountain Maneuvers with a Bioinspired Underwater Robot Collective

Florian Berlinger, Paula Wulkop, and Radhika Nagpal

**Abstract**—Several animal species self-organize into large groups to leverage vital behaviors such as foraging, construction, or predator evasion. With the advancement of robotics and automation, engineered multi-agent systems have been inspired to achieve similarly high degrees of scalable, robust, and adaptable autonomy through decentralized and dynamic coordination. So far however, they have been most successfully demonstrated above ground or with partial assistance from central controllers and external tracking. Here we demonstrate an underwater robot collective that realizes full spatiotemporal coordination. Using the example of fish-inspired evasive maneuvers, our robots display alignment, formation control, and coordinated escape, enabled by real-time on-board multi-robot tracking and local decision making. Accompanied by a custom simulator, this robotic platform advances the physically-validated development of algorithms for collective behaviors and future applications including collective exploration, tracking and capture, or environmental sampling.

## I. INTRODUCTION

Predation plays an important role in balancing ecosystems and is one driver of evolution, which pushes animal populations toward those individuals or groups which have evolved successful escape strategies [1], [2]. Such escape can be witnessed from tiny plankton [3] to bird flocks [4] and fish schools [5], [6]. Particularly impressive are social preys that cooperate through local interactions to evade predators collectively. Fish, for example, display several evasive behaviors, ranging from the fountain maneuver [5], [6] to flash expansion and bait balls [7]. In doing so, schooling fish demonstrate collective vigilance and resilience that leverages the cognition and actions of all individuals [5], [6].

For robotic swarms, the ability to escape threats or moving obstacles exemplifies complex dynamic coordination that goes beyond simple and well-studied flocking [8], [9], [10]. With such coordination, a group of underwater robots deployed to monitor coastal environments like coral reefs and harbors, could, for instance, react cohesively to circumnavigate oncoming traffic. Similar maneuvers would also be useful for aerial drone swarms. Current aerial swarms, however, typically still rely on assistive technologies such as centralized base stations, motion capture, and the global positioning system (GPS) [11], [12], [13], [14], [15], [16]. These technologies may be unavailable to underwater collectives,

This work was supported by the Office of Naval Research (ONR Award No.: N00014-20-1-2320), the Wyss Institute for Biologically Inspired Engineering, and an Amazon AWS Research Award.

The supplementary material is available at [https://bit.ly/evasive\\_maneuvers](https://bit.ly/evasive_maneuvers).

The authors were with the John A. Paulson School of Engineering and Applied Science at Harvard University, Cambridge, Massachusetts. E-mails: {fberlinger, nagpal}@g.harvard.edu, pwulkop@ethz.ch.

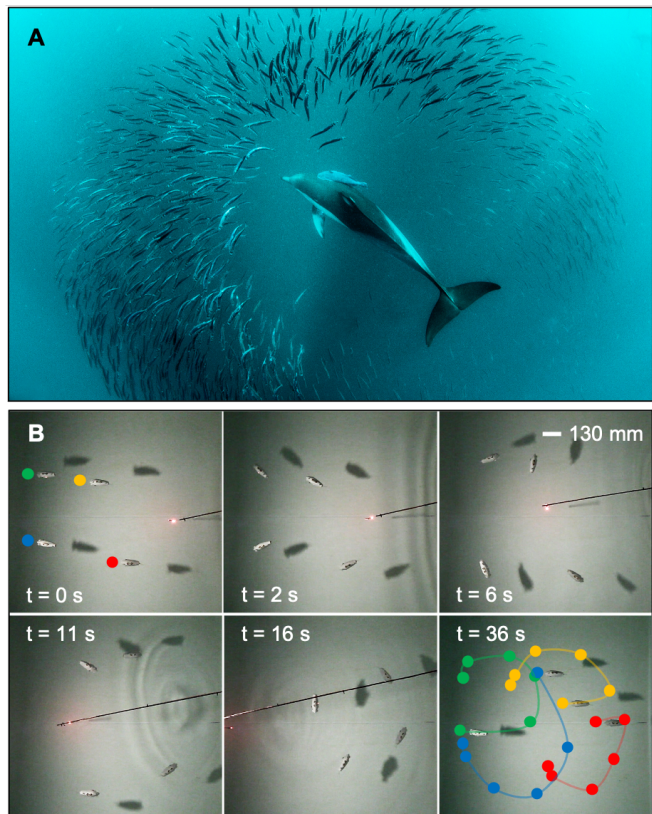


Fig. 1. **Evasive maneuvers.** (A) A fish shoal reacts to a predatory dolphin by performing a fountain maneuver (credit: iStock). (B) Four Bluebots (130 mm in length) react to a manually guided predator surrogate. Initially self-aligned and facing to the left ( $t = 0$  s), the robots embark on fountain-shaped trajectories to evade the predator, which inadvertently moves through the middle of the shoal ( $t = 2$  s until  $t = 16$  s). Once the danger has passed, the Bluebots regroup and realign ( $t = 36$  s). Color-coded initial positions and trajectories were added to the top left and bottom right snapshots.

which further restrains their coordination [17], [18], [19], [20]. Overall, robotic swarms have not been able to reproduce the high degree of scalable, robust, and adaptable autonomy that natural systems achieve through self-organization [21].

To narrow this gap, we aimed to mimic the dynamic and parallel coordination of fish during predator attacks (Figure 1) with an underwater robot collective, using the example of the fountain maneuver [5], [6]. When a fish school performs a fountain maneuver, the fish typically encircle the predator and reunite behind it, taking advantage of its high inertia and letting it swim through the void. Many fish species use visual observations of nearby neighbors [22], [23], [24], [25], [26] and have evolved specialized visual patterns called schooling marks [27] for such group coordination

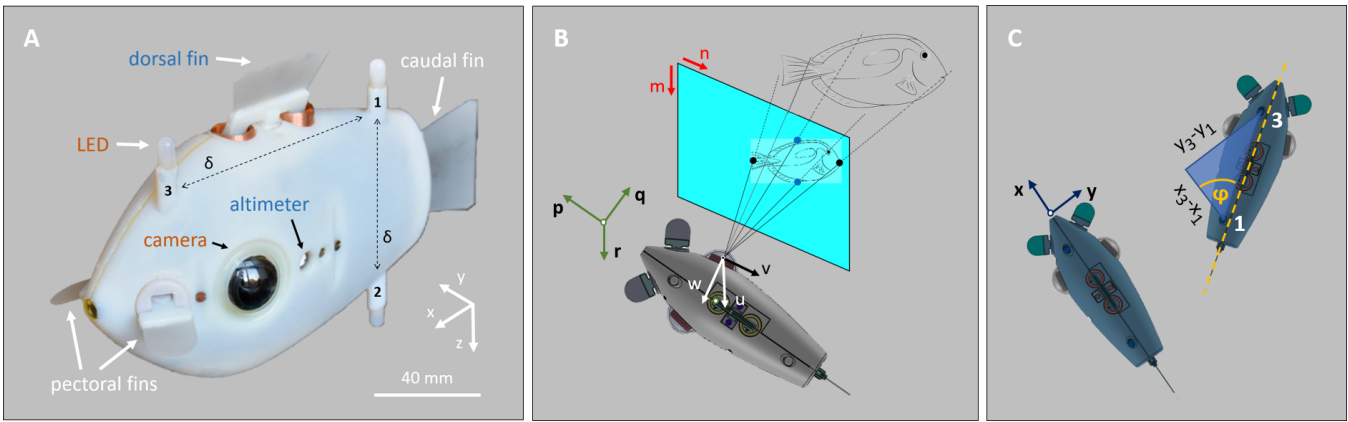


Fig. 2. **Blueswarm platform.** (A) Autonomous multi-fin locomotion is guided by real-time on-board sensing and processing of neighboring robots (cameras and LEDs) and diving depth (altimeter). (B) To infer the direction in which an object is observed, individual LED blobs are identified in the  $mn$  image plane, their centroids projected onto a camera-based  $uvw$  unit sphere, and then aligned with the  $pqr$  coordinate frame attached to the robot's center of mass. The distance in scaled  $xyz$  coordinates to such object can be found from two object points, whose real-world distance is known, e.g., the vertical posterior LEDs 1 and 2 of a Bluebot, which are  $\delta = 86$  mm apart. (C) The *relative heading*  $\varphi$  can be found from a non-aligned third object point, e.g., the anterior LED 3, which is in the same horizontal plane and at a distance of  $\delta = 86$  mm from LED 1.

that involves alignment before and dynamic evasion during an attack. Remarkably, many schooling behaviors including predator evasion work with limited and decentralized coordination as opposed to any one single fish permanently leading the school [21], [28], [29], [30].

Inspired by the coordination among fish, our Bluebot robots (Figure 2A) have three blue-light LEDs as visual beacons for camera-based neighbor detection [31]. This enables preprogrammed local decisions for collective actions without the need for any assistive technologies. Due to their three-dimensional (3D) multi-fin locomotion and visual perception, Bluebots are a versatile swarm robotic platform to investigate self-organized collective behaviors [31], as well as laboratory surrogates to study biomimetic actuation methods [32], [33] and fish swimming [34], [35].

The two principal contributions of this paper are: (i) The algorithmic design and experimental validation of the fountain maneuver on physical underwater robots, using only local autonomous interactions. In order to achieve this, we implemented a camera-LED vision system for the rapid inference of position, distance, and heading of neighboring robots. (ii) A study of the robustness and scalability of the fountain maneuver across several dimensions. This study is enabled through the design of a realistic Blueswarm simulator that can be used to investigate the gaps between ideal systems and hardware constraints.

## II. RELATED WORK

A wealth of experimental and theoretical work exists on flocking and alignment as it is observed in fish schools [36], [37], [38], [39], [40]. Biologists have described several advantages of schooling – among them protection from predatory attacks – and documented a range of evasive maneuvers [5], [6], [22]. Which maneuver fish choose depends on the direction of the attack [41]; split behavior like the fountain maneuver is triggered by attacks from behind. In contrast, the local mechanisms for evasive behaviors have

been less well understood. Only a single descriptive model of the fountain maneuver exists and proposes that fish visually monitor the predator to maximize the rate of escape while minimizing the associated energetic cost [42]. To do so, fish are assumed to swim away from the predator at a constant angle determined by the rear limit of their visual field. This model was confirmed in tests with juvenile whittings [42], and served as the basis for the evasion part of our experiments.

In the robotics domain, very few examples exist of implementing bioinspired evasive maneuvers. Fish-inspired escape was demonstrated with centrally-controlled ground robots [43], and variations of flash expansion and fountain maneuvers were implemented for obstacle avoidance with LEGO robots [44]. In computer graphics, animations of the fountain maneuver were created, however the underlying algorithms used global knowledge that would not be available to fish or robots [45]. In contrast to evasive behaviors, basic heading alignment has been well studied; collective alignment can be achieved with simple averaging algorithms [46] and was shown with ground-based robots that use local perception to detect neighbor headings [47] and with aerial robots that exchange GPS headings wirelessly [14].

To the best of our knowledge, we present the first demonstration of the fountain maneuver with an autonomous underwater robot collective, using only local visual perception and interactions. In contrast to previous work [42], [45], we present a fully decentralized algorithm that includes all aspects of the fountain maneuver (alignment, detection, evasion, regroup). Furthermore, we physically validate our collective algorithm on Blueswarm, using only local interactions and no global assistance on GPS or motion capture [11], [12], [13], [14], [15], [16], [17], [18], [19], [20].

## III. BLUESWARM PLATFORM

Blueswarm is a 3D underwater robot collective that uses local vision-based coordination to self-organize. Here we focus on a few of Blueswarm's essential and previously

introduced features [31], as well as two new aspects: (i) the ability for robots to visually sense neighbor headings; (ii) a hardware-specific simulation platform for wider exploration.

#### A. Robot design and visual inference of headings

Bluebots have four independently controllable fins to move in 3D space; the dorsal fin and feedback from an altimeter are used for vertical diving exclusively [48]. Two cameras cover a near-omnidirectional field of view, in which neighboring robots are tracked by their three blue light LEDs (Figure 2A). To infer the relative position, distance, and heading to a neighboring robot, the scenery of observed LEDs has to be parsed to identify LED triplets belonging to individual robots (Section IV). Since Bluebots are passively stable in roll and pitch, their posterior LEDs remain stacked vertically and their upper LEDs remain in a horizontal plane. The posterior LEDs were used previously to infer distance to neighboring robots [31]. The anterior LED was added for this work, allowing the calculation of the *relative heading*  $\varphi$  of a neighboring robot via projective geometry (Figure 2B-C). The calculation finds a scaling factor  $\lambda$  to go from the normalized *pqr* direction in which the neighboring robot is observed to the scaled *xyz* real-world coordinates of the anterior LED 3 of that robot:

$$\lambda(p_3, q_3, r_3) = (x_3, y_3, z_3).$$

It uses the fact that LED 3 is on a horizontal circle of radius  $\delta = 86$  mm around the upper posterior LED 1, whose position  $(x_1, y_1, z_1)$  is known from the distance estimate [31]:

$$(\lambda p_3 - x_1)^2 + (\lambda q_3 - y_1)^2 = \delta^2. \quad (1)$$

Eq. 1 can be solved for  $\lambda$  with the quadratic formula. The  $\lambda$  is selected for which  $|z_1 - z_3|$  is smaller, since LEDs 1 and 3 are in the same horizontal plane. Given the *xyz* coordinates of LEDs 1 and 3, the relative heading  $\varphi$  of the neighboring robot follows from Figure 2C (Eq. 2):

$$\varphi = \text{atan2} \left( \frac{y_3 - y_1}{x_3 - x_1} \right). \quad (2)$$

#### B. Testing environments and predator

We ran experiments at two different test sites. Our in-house testing environment is a square water tank of size  $1.78 \times 1.78 \times 1.17$  meters or  $13.7 \times 13.7 \times 9.0$  body lengths (henceforth the *small tank*). A larger circular water tank at the Olin College of Engineering had a diameter of 6.1 m and a depth of 1.5 m (henceforth the *large tank*). As a predator, we used two vertically stacked red LEDs on rod that was moved by a human.

#### C. Simulator design

In order to analyze and improve the robustness and scalability of our implementations for evasive maneuvers, we built a custom simulator. Named Bluesim, that simulator closely matches the locomotion and perception of Bluebots. In Bluesim, a central database keeps track of positions, velocities, relative positions, and distances of all simulated

robots. To capture the asynchrony and perception-cognition-action cycle duration (0.5 s) of the robots, we use the following process: In each simulation step, a robot exits a heap, perceives its neighbors and executes its move, updates its state in the central database, and re-enters the heap. The heap is sorted according to an arrival process, with robots drawing normal deviates with means equivalent to the expected duration (0.5 s).

The dynamics of Bluebot were modelled as a non-linear time-invariant system, and its motion expressed as a set of second order differential equations. We simulate Bluebot's motion by solving these equations continuously using Euler integration. Shown here is the equation describing translational motions along Bluebot's *x*-axis (Eq. 3); translational motions along the *y*- and *z*-axes, as well as rotations around the *z*-axis follow accordingly (supplement section 1.1):

$$\ddot{x} = \frac{1}{m} \left( \underbrace{F_{caud} - \sin \gamma_{pect} (F_{PL} + F_{PR})}_{\text{thrust}} - \underbrace{\frac{1}{2} \rho c_{dx} A_x \text{sgn}(\dot{x}) \dot{x}^2}_{\text{drag}} \right), \quad (3)$$

with known pectoral angle  $\gamma_{pect} = \pi/6$ , and water density  $\rho = 998$  kg/m<sup>3</sup>; estimated robot inertial mass  $m = 0.5$  kg (incl. added mass), robot drag coefficient  $c_{dx} = 0.5$  (cf. cone), and reference area  $A_x = 3.14 \times 10^{-3}$  m<sup>2</sup>; and empirically found thrust forces for caudal ( $F_{caud}$ ) and pectoral left ( $F_{PL}$ ) and right ( $F_{PR}$ ) fins. The fin forces vary with their actuation frequencies, and reach up to 20 mN for the caudal and dorsal fins, and 6 mN for each pectoral fin (resulting in a maximum forward speed of 160 mm/s or 1.23 body lengths per second).

The perception of Bluebot was replicated by simulating its visual range (3 m) and narrow posterior blind spot (a 50 mm wide corridor), as well as neighbor occlusions (supplement section 1.2). For occlusions, each robot was geometrically simplified as a visually blocking sphere of radius 50 mm that forms the upper base of a blocking conical frustum. Robots outside the visual range, inside the blind spot, or hidden behind another robot get removed from the set of neighbors taken into account for local decision making. For the remaining robots, positional information can be returned in two ways: (i) at the robot level with perfect or noisy relative distance and heading; (ii) at the LED level including reflections at the water surface, which allows for the testing of LED parsing and tracking algorithms.

## IV. BEHAVIORAL MODELLING

As part of a fountain maneuver, fish typically encircle a predator and realign behind it (Figure 1). We modelled the fountain maneuver triggered by a predatory attack as a finite-state machine: robots start in the *Align* state and transition into the *Evade* state if they *Detect* a predator (Figure 3).

#### A. Align

During alignment, Bluebots detect and track neighboring robots to infer their headings and rotate toward the un-weighted average heading. Following this simple averaging

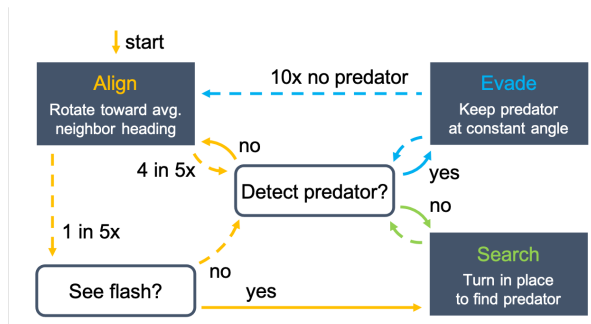


Fig. 3. **Fountain maneuver finite-state machine.** Yellow loop: Bluebots transition from the *Align* into the *Evade* state if they detect a predator, or the *Search* state if they see a flashing neighbor (checked in every fifth iteration). Green loop: Flash-alerted Bluebots remain in the *Search* state until they detect the predator themselves and switch into the *Evade* state. Blue loop: Bluebots transition from the *Evade* back into the *Align* state if they do not detect the predator for ten consecutive iterations.

protocol, a convergence proof (by induction) is straightforward under the assumption of accurate and fast enough perception and locomotion that lead to monotonically decreasing deviations in robot headings [46]. Our experiments provide insight into how robustly alignment works with Bluebots’ imperfect inference of headings, and how tight a convergence bound can be achieved. We used a Kalman filter to improve the parsing of LEDs and tracking of neighboring robots by estimation of their positions as opposed to our previous work [31], which did not make use of historical observations.

### B. Detect

In order to distinguish the predator (two red LEDs) from fellow robots (three blue LEDs), a Bluebot derives the red-to-blue ratio of all LED blobs. A predator is detected if any two blobs have such a ratio greater than 1.2 and are vertically stacked (from which the distance is known as well). A Bluebot then stops aligning and starts evading the predator.

In addition, Bluebots that have detected a predator can flash their LEDs (at 15 Hz) to alert fellow robots, programmed to check for flashing in a series of 30 images taken in burst mode at 60 frames-per-second. Similar flashing alerts were observed in schools of anchovy, which roll their bodies to reflect sunlight off their shiny silver ventral sides [49].

The flashing signal as well as the distinction of LED colors have been used in our previous work [31]. Here we tuned both to lean toward false negatives such that evasion is not triggered accidentally.

### C. Evade

Inspired by a descriptive model of the fountain maneuver [42], Bluebots evade a predator by swimming away while keeping it visible at a constant angle of  $|\pm 60^\circ|$ . The result is a fountain-shaped trajectory. Bluebots detecting the predator to their right (or left) evade in counterclockwise (or clockwise) direction, using proportional control and the caudal and pectoral right (or left) fin. Once the predator can no longer be seen, Bluebots complete the maneuver by going back to alignment. We added hysteresis to provide robustness against sporadic misses of the predator (i.e., false negatives

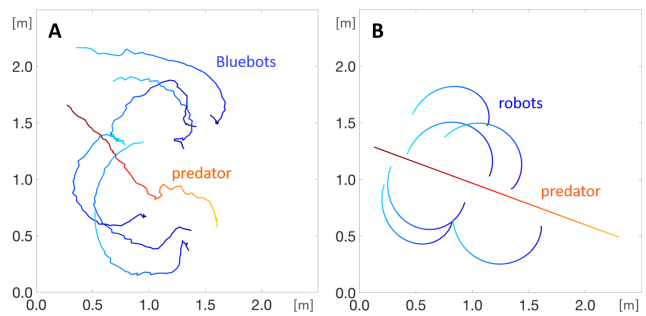


Fig. 4. **Fountain maneuver trajectories.** (A) Tracked from an experiment with six Bluebots in the large tank. (B) Plotted from a simulation with six robots. (A,B) Time (0 s – 27.5 s) indicated by color progression from dark (early) to light (late); robots in blue, predator in red. Shown in the supplemental movie.

due to occlusions), which would result in premature (and potentially fatal) abandonment of evasion.

## V. EXPERIMENTAL RESULTS

In experiments with Blueswarm, we demonstrated that self-organized fountain maneuvers are feasible despite limited perception quality and cognition speed paired with submerged but imperfect motion (Figures 1B and 4-5 and supplemental movie). Simulations allowed us to repeat experiments to statistically analyze robustness and scalability, as well as to inform and refine algorithmic implementations for the physical-robot experiments (Figures 6-8).

When fish escape during a fountain maneuver, they dart away from the aligned school to keep the predator at a safe distance and within their visual field [42]. Accordingly, the three key metrics for Bluebots were: (i) stable alignment with circular standard deviations  $\sigma_\phi \leq 0.5$ ; (ii) convergence to a prescribed viewing angle  $\Theta$  at which the predator is kept; (iii) increased distance  $d$  to the predator compared to not taking action. Although this behavior has been described extensively in fish literature [5], [6], [7], [42], it is mostly studied qualitatively without standard metrics for quantification.

### A. The fountain maneuver with physical robots

The fountain maneuver can be split into two main dynamic parts: *Align* and *Evade*. Alignment allows Bluebots to move from a shoaling into a schooling state, enhancing collective order and preparing the school for effective predator evasion. As such, the behavior is also useful for formation control, for example to migrate long distances efficiently. In two experiments (red, blue) in the large tank, seven Bluebots aligned their *absolute* headings  $\phi$  after approximately 15 to 20 seconds, and achieved final average circular standard deviations  $\sigma_\phi$  of 0.29 and 0.30, respectively (Figure 5A-B and supplemental movie). During alignment, Bluebots detected 2.14 (red) and 2.19 (blue) neighboring robots on average (supplement section 2.1). Alignment did not improve neighbor visibility. This suggests that visual interactions may be equally noisy in both aligned configurations (schooling) and non-aligned configurations (shoaling).

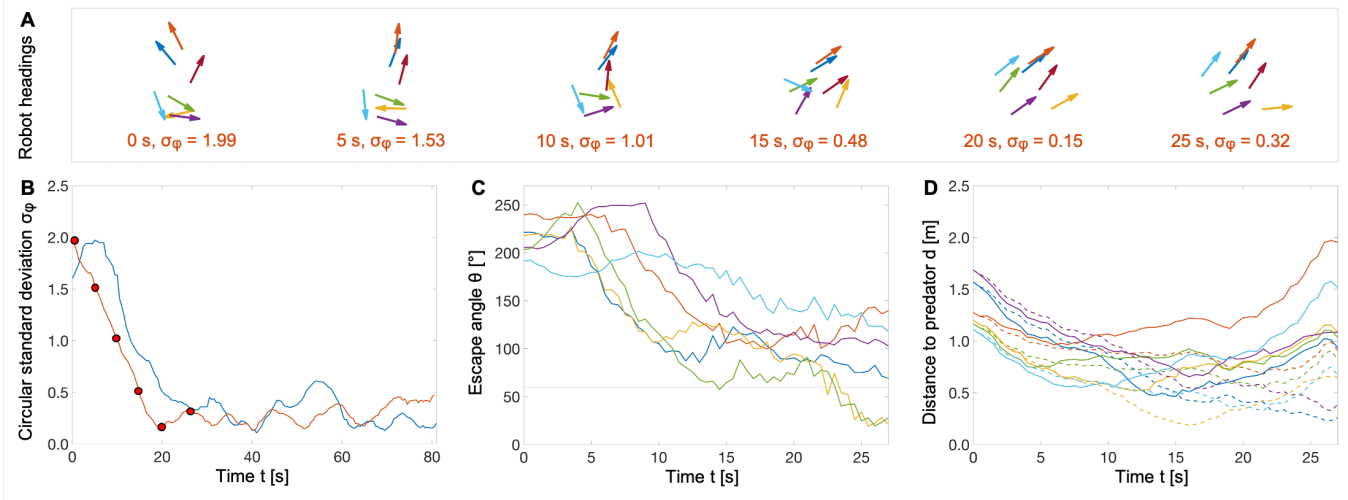


Fig. 5. **Blueswarm escapes the predator (hardware experiments).** (A-B) Alignment with seven Bluebots: The circular standard deviations  $\sigma_\phi$  of the headings converged to means of 0.29 (red) and 0.30 (blue) after approximately 15 to 20 seconds. (A) shows individual headings during the red experiment at times marked in (B). (C-D) Escape with six Bluebots (color-coded): (C) Escape angles  $\Theta$  approached  $60^\circ$  (dashed line) during the fountain maneuver; (D) Distances  $d$  to the predator were effectively increased by active evasion (solid lines) compared to remaining idle at the initial position (dashed lines).

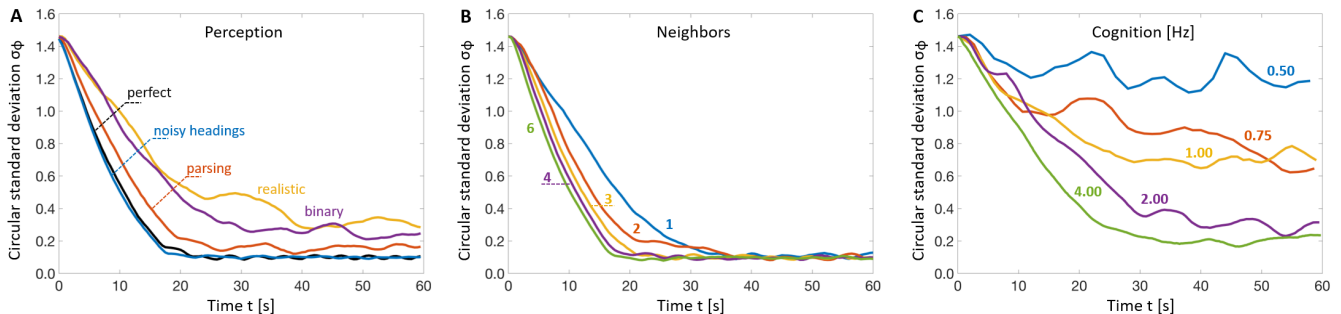


Fig. 6. **Robustness of alignment with seven simulated robots.** (A) Perception quality matters critically for alignment. Black: perfect perception; blue: noisy headings with  $\mathcal{N}(\mu = 0, \sigma = 10^\circ)$ ; red: noisy headings and parsing; yellow: noisy headings, noisy LEDs with  $\mathcal{N}(\mu = 0, \sigma = 2\text{mm})$ , and parsing (realistic Bluebot perception); purple: noisy headings, noisy LEDs, parsing, and reduction to binary directions (heading right/left). (B) Alignment works robustly, regardless of the number of visible robots, but takes longer with fewer visible robots. (C) Faster cognition results in faster alignment. Cognition speeds below 1 Hz impede the convergence of headings. All data points were averaged across  $N = 10$  simulation runs.

Bluebot trajectories during the evasion part resembled the fountain maneuver (Figure 4A). The robots rotated away from the predator and approached the prescribed  $|60^\circ|$  escape angle  $\Theta$  (Figure 5C), by which they increased the minimal distance from the predator by 156% (Figure 5D) as opposed to when they remained idle at their initial positions. Further analysis is available in supplement sections 2.2-2.3.

### B. Robustness and scalability from simulation

In order to provide insight into the robustness and scalability of the fountain maneuver, we complemented robot demonstrations with simulations. We varied perception quality, neighbor visibility, cognition speed, and number of robots during alignment, and simulated different escape angles  $\Theta$ .

1) *Perception quality*: Alignment relies on the accurate detection of neighbor headings. In simulation, we compared alignment with perfect perception against realistic perception, modelled after Bluebot and including noisy estimates for LED positions and robot headings (zero-mean Gaussians with standard deviations of 2 mm and  $10^\circ$ , respectively), as

well as imperfect LED parsing. This realistic perception was used for the cognition and scalability simulations; alternative noise magnitudes are shown in section 2.4 of the supplement. As expected, we found that LED position errors are more severe than noisy headings (Figure 6A), since parsing relies on the heuristic that the posterior LEDs are stacked vertically, and wrongly parsed robot LEDs introduce arbitrary headings. Interestingly, simulation indicates that precise heading information is not required for alignment: convergence with realistic perception was similarly good, even when inferred headings were reduced to binary information on whether another robot is facing to the right ( $0^\circ \leq \phi < 180^\circ$ ) or left ( $180^\circ \leq \phi < 360^\circ$ ). Alignment started to break down, however, if noise levels on robot headings or LED positions exceeded  $20^\circ$  or 2 mm, or the probability of parsing errors was higher than 10% (supplement section 2.4).

2) *Neighbor visibility*: During alignment with seven robots, Bluebots detected approximately 2.2 out of 6 possible neighbors on average with expected loss due to occlusion, occasional misidentified robots, and information loss during

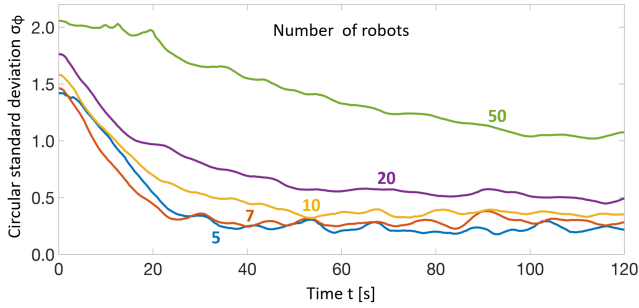


Fig. 7. **Scalability of alignment.** Convergence of headings takes longer and settles at higher circular standard deviations  $\sigma_\phi$  with an increasing number of robots. All data points were averaged across  $N = 10$  simulation runs.

conservative parsing (supplement section 2.1). In simulations with seven robots, we assigned a random subset of visible neighbors to each robot in each iteration, and compared the effect of the subset size on alignment. In this case, there was no parsing and no noise on the LED positions. The convergence of robot headings was accelerated if more than 2.2 neighbors were visible; conversely, it slowed down and almost doubles if one single neighbor was visible only (Figure 6B). The final circular standard deviation  $\sigma_\phi$  was unaffected by the number of visible neighbors. As with schooling fish that exhibit group-level coordination, a limited [25], [29] and noisy [50] count of neighbors was sufficient to achieve alignment consensus in our experiments.

3) *Cognition speed:* Faster cognition – achievable with more powerful hardware or more performant algorithms – allows for more frequent sensing, which generally results in more accurate state estimation and control. Bluebots’ cognition speed is most severely affected by the complexity of image processing. Average sensing iteration frequencies of 3.42 Hz were measured during alignment only, and dropped to 0.96 Hz when predator detection was added. Simulations with seven robots showed that the quality of alignment deteriorates for frequencies below 1 Hz (Figure 6C). This prevented us from using a previously developed [31] and bioinspired [49] flashing mechanism to warn fellow Bluebots against the predator; while effective for predator alert (supplemental movie), flash detection slowed down and damaged alignment significantly.

4) *Number of robots:* We simulated alignment with 5–50 robots to assess whether our implementation scales well to larger collectives. Perception and cognition of these simulated robots matched the Bluebots. For headings, the convergence time grew and the final circular standard deviation  $\sigma_\phi$  deteriorated with the number of robots (Figure 7). This confirms our expectation that with more robots, occlusions become more frequent and inferring individual headings more challenging. As a result, small alignment errors add up from one end of the collective to another.

5) *Escape angle:* The fountain maneuver grows with the escape angle  $\Theta$  (Figure 8);  $|\Theta = 60^\circ|$  was chosen for physical experiments due to space constraints in our testing environments. In comparison, the same maneuver with  $|\Theta = 150^\circ|$  –

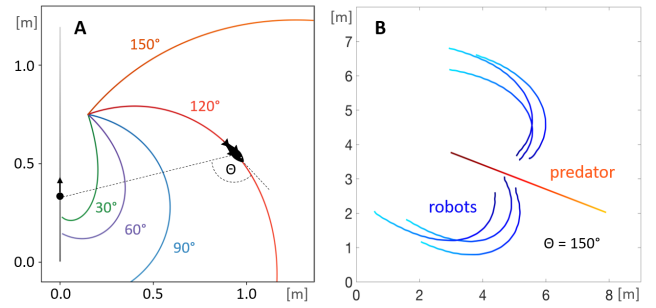


Fig. 8. **Escape angles.** (A) The larger the escape angle  $\Theta$ , the longer are the escape trajectories (colored). The predator moves from bottom to top and is indicated by the vertical line on the left (greyscale). (B) A fountain maneuver with six simulated robots and an escape angle of  $|\Theta = 150^\circ|$ .

the rear limit of the visual field of gadoid fish [42] – requires nearly ten times as much space (compare Figures 8B and 4B). Simulated robots were able to reach and hold larger escape angles more easily (supplement section 2.2).

## VI. CONCLUSIONS AND FUTURE WORK

We designed, implemented, and demonstrated the fountain maneuver on the Blueswarm platform. Qualitative experiments with Bluebots (Figures 1B and 4-5) proved that our algorithms are robust enough for physical demonstrations despite limitations on perception (non-visible neighbors due to blind spots and occlusions) and cognition (limited image processing speed and tracking errors). Quantitative experiments in simulation (Figures 6-8) revealed that fast and reliable neighbor tracking matters critically for alignment. However, exact headings do not seem to be required.

The fountain maneuvers demonstrated here were more dynamic and perceptually complex than previous 3D behaviors with Blueswarm [31] by using the anterior LED to infer and coordinate heading with neighbors. Our results show that by careful integration of hardware (especially cameras and LEDs) and software (especially image processing and neighbor tracking), self-organized and dynamic collective behaviors are possible on completely autonomous, unassisted, and miniature underwater robots.

With the current on-board compute power, we were constrained to asking a single question from every image (e.g., neighbor positions *or* flashing neighbors) to achieve high enough perception-cognition-action cycle frequencies. Moreover, our vision algorithms relied on a clear and dark water environment for the detection of LED blobs. In the future, we envision robots with enhanced compute power, able to detect other robots in front of varied and dynamic backgrounds. Such a collective could coordinate without active (i.e., LED) visual markers and more easily navigate in real-world environments like aquariums, coral reefs, or harbors for collective patrolling, sampling, and search.

## ACKNOWLEDGMENTS

We thank Prof. Jeff Dusek for providing access to a testing pool at the Olin College of Engineering, and Dr. Nicholas Lawrance and Fritz Lekschas for helpful discussions.

## REFERENCES

- [1] A. A. Berryman, "The origins and evolution of predator-prey theory," *Ecology*, vol. 73, no. 5, pp. 1530–1535, 1992.
- [2] T. Yoshida, L. E. Jones, S. P. Ellner, G. F. Fussmann, and N. G. Hairston, "Rapid evolution drives ecological dynamics in a predator-prey system," *Nature*, vol. 424, no. 6946, pp. 303–306, 2003.
- [3] T. M. Zaret and J. S. Suffern, "Vertical migration in zooplankton as a predator avoidance mechanism 1," *Limnology and oceanography*, vol. 21, no. 6, pp. 804–813, 1976.
- [4] C. L. Devereux, M. J. Whittingham, E. Fernández-Juricic, J. A. Vickery, and J. R. Krebs, "Predator detection and avoidance by starlings under differing scenarios of predation risk," *Behavioral Ecology*, vol. 17, no. 2, pp. 303–309, 2006.
- [5] B. L. Partridge, "The structure and function of fish schools," *Scientific american*, vol. 246, no. 6, pp. 114–123, 1982.
- [6] E. Shaw, "Schooling fishes: the school, a truly egalitarian form of organization in which all members of the group are alike in influence, offers substantial benefits to its participants," *American Scientist*, vol. 66, no. 2, pp. 166–175, 1978.
- [7] T. J. Pitcher and C. J. Wyche, "Predator-avoidance behaviours of sandeel schools: why schools seldom split," in *Predators and prey in fishes*. Springer, 1983, pp. 193–204.
- [8] R. Olfati-Saber, "Flocking for multi-agent dynamic systems: Algorithms and theory," *IEEE Transactions on automatic control*, vol. 51, no. 3, pp. 401–420, 2006.
- [9] H. G. Tanner, A. Jadbabaie, and G. J. Pappas, "Stable flocking of mobile agents, part i: Fixed topology," in *42nd IEEE International Conference on Decision and Control (IEEE Cat. No. 03CH37475)*, vol. 2. IEEE, 2003, pp. 2010–2015.
- [10] N. Moshtagh and A. Jadbabaie, "Distributed geodesic control laws for flocking of nonholonomic agents," *IEEE Transactions on Automatic Control*, vol. 52, no. 4, pp. 681–686, 2007.
- [11] J. A. Preiss, W. Honig, G. S. Sukhatme, and N. Ayanian, "Crazyswarm: A large nano-quadcopter swarm," in *2017 IEEE International Conference on Robotics and Automation (ICRA)*. IEEE, 2017, pp. 3299–3304.
- [12] A. Kushleyev, D. Mellinger, C. Powers, and V. Kumar, "Towards a swarm of agile micro quadrotors," *Autonomous Robots*, vol. 35, no. 4, pp. 287–300, 2013.
- [13] A. Weinstein, A. Cho, G. Loianno, and V. Kumar, "Visual inertial odometry swarm: An autonomous swarm of vision-based quadrotors," *IEEE Robotics and Automation Letters*, vol. 3, no. 3, pp. 1801–1807, 2018.
- [14] G. Vásárhelyi, C. Virágh, G. Somorjai, T. Nepusz, A. E. Eiben, and T. Vicsek, "Optimized flocking of autonomous drones in confined environments," *Science Robotics*, vol. 3, no. 20, 2018.
- [15] S. Hauert, S. Leven, M. Varga, F. Ruini, A. Cangelosi, J.-C. Zufferey, and D. Floreano, "Reynolds flocking in reality with fixed-wing robots: communication range vs. maximum turning rate," in *2011 IEEE/RSJ International Conference on Intelligent Robots and Systems*. IEEE, 2011, pp. 5015–5020.
- [16] K. McGuire, C. De Wagter, K. Tuyls, H. Kappen, and G. C. de Croon, "Minimal navigation solution for a swarm of tiny flying robots to explore an unknown environment," *Science Robotics*, vol. 4, no. 35, p. eaaw9710, 2019.
- [17] P. Zahadat and T. Schmickl, "Division of labor in a swarm of autonomous underwater robots by improved partitioning social inhibition," *Adaptive Behavior*, vol. 24, no. 2, pp. 87–101, 2016.
- [18] T. Schmickl, R. Thenius, C. Moslinger, J. Timmis, A. Tyrrell, M. Read, J. Hilder, J. Halloy, A. Campo, C. Stefanini *et al.*, "Cocoro—the self-aware underwater swarm," in *2011 Fifth IEEE Conference on Self-Adaptive and Self-Organizing Systems Workshops*. IEEE, 2011, pp. 120–126.
- [19] N. E. Leonard, D. A. Paley, R. E. Davis, D. M. Fratantoni, F. Lekien, and F. Zhang, "Coordinated control of an underwater glider fleet in an adaptive ocean sampling field experiment in monterey bay," *Journal of Field Robotics*, vol. 27, no. 6, pp. 718–740, 2010.
- [20] J. S. Jaffe, P. J. Franks, P. L. Roberts, D. Mirza, C. Schurgers, R. Kastner, and A. Boch, "A swarm of autonomous miniature underwater robot drifters for exploring submesoscale ocean dynamics," *Nature communications*, vol. 8, no. 1, pp. 1–8, 2017.
- [21] S. Camazine, J.-L. Deneubourg, N. R. Franks, J. Sneyd, E. Bonabeau, and G. Theraula, *Self-organization in biological systems*. Princeton university press, 2003.
- [22] T. J. Pitcher, "Functions of shoaling behaviour in teleosts," in *The behaviour of teleost fishes*. Springer, 1986, pp. 294–337.
- [23] R. H. Douglas and C. W. Hawryshyn, "Behavioural studies of fish vision: an analysis of visual capabilities," in *The visual system of fish*. Springer, 1990, pp. 373–418.
- [24] B. L. Partridge and T. J. Pitcher, "The sensory basis of fish schools: relative roles of lateral line and vision," *Journal of comparative physiology*, vol. 135, no. 4, pp. 315–325, 1980.
- [25] L. Jiang, L. Giuggioli, A. Perna, R. Escobedo, V. Lecheval, C. Sire, Z. Han, and G. Theraulaz, "Identifying influential neighbors in animal flocking," *PLoS computational biology*, vol. 13, no. 11, p. e1005822, 2017.
- [26] J. R. Stowers, M. Hofbauer, R. Bastien, J. Griessner, P. Higgins, S. Farooqui, R. M. Fischer, K. Nowikovsky, W. Haubensack, I. D. Couzin *et al.*, "Virtual reality for freely moving animals," *Nature methods*, vol. 14, no. 10, pp. 995–1002, 2017.
- [27] Q. Bone and R. Moore, *Biology of fishes*. Taylor & Francis, 2008.
- [28] J. K. Parrish, S. V. Viscido, and D. Grunbaum, "Self-organized fish schools: an examination of emergent properties," *The biological bulletin*, vol. 202, no. 3, pp. 296–305, 2002.
- [29] I. D. Couzin, J. Krause, N. R. Franks, and S. A. Levin, "Effective leadership and decision-making in animal groups on the move," *Nature*, vol. 433, no. 7025, pp. 513–516, 2005.
- [30] J. Krause, D. Hoare, S. Krause, C. Hemelrijk, and D. Rubenstein, "Leadership in fish shoals," *Fish and Fisheries*, vol. 1, no. 1, pp. 82–89, 2000.
- [31] F. Berlinger, M. Gauci, and R. Nagpal, "Implicit coordination for 3d underwater collective behaviors in a fish-inspired robot swarm," *Science Robotics*, vol. 6, no. 50, 2021.
- [32] K. Soltan, J. O'Brien, J. Dusek, F. Berlinger, and R. Nagpal, "Biomimetic actuation method for a miniature, low-cost multi-jointed robotic fish," in *OCEANS 2018 MTS/IEEE Charleston*. IEEE, 2018, pp. 1–9.
- [33] F. Berlinger, M. Duduta, H. Gloria, D. Clarke, R. Nagpal, and R. Wood, "A modular dielectric elastomer actuator to drive miniature autonomous underwater vehicles," in *2018 IEEE International Conference on Robotics and Automation (ICRA)*. IEEE, 2018, pp. 3429–3435.
- [34] F. Berlinger, M. Saadat, H. Haj-Hariri, G. Lauder, and R. Nagpal, "An autonomous, multi-fin, and biomimetic robot for three-dimensional fish-like swimming," *Bioinspiration and Biomimetics*, (in revision).
- [35] M. Saadat, F. Berlinger, A. Sheshmani, R. Nagpal, G. Lauder, and H. Haj-Hariri, "Hydrodynamic advantages of in-line schooling," *Bioinspiration and Biomimetics*, (in revision).
- [36] C. W. Reynolds, "Flocks, herds and schools: A distributed behavioral model," in *Proceedings of the 14th annual conference on Computer graphics and interactive techniques*, 1987, pp. 25–34.
- [37] T. Vicsek, A. Czirók, E. Ben-Jacob, I. Cohen, and O. Shochet, "Novel type of phase transition in a system of self-driven particles," *Physical review letters*, vol. 75, no. 6, p. 1226, 1995.
- [38] D. S. Calovi, A. Litchinko, V. Lecheval, U. Lopez, A. P. Escudero, H. Chaté, C. Sire, and G. Theraulaz, "Disentangling and modeling interactions in fish with burst-and-coast swimming reveal distinct alignment and attraction behaviors," *PLoS computational biology*, vol. 14, no. 1, p. e1005933, 2018.
- [39] M. Adiou, J. Treuil, and O. Arino, "Alignment in a fish school: a mixed lagrangian–eulerian approach," *Ecological Modelling*, vol. 167, no. 1–2, pp. 19–32, 2003.
- [40] E. Carlen, M. C. Carvalho, P. Degond, and B. Wennberg, "A boltzmann model for rod alignment and schooling fish," *Nonlinearity*, vol. 28, no. 6, p. 1783, 2015.
- [41] S. Marras, R. S. Batty, and P. Domenici, "Information transfer and antipredator maneuvers in schooling herring," *Adaptive Behavior*, vol. 20, no. 1, pp. 44–56, 2012.
- [42] S. Hall, C. Wardle, and D. MacLennan, "Predator evasion in a fish school: test of a model for the fountain effect," *Marine biology*, vol. 91, no. 1, pp. 143–148, 1986.
- [43] H. Min and Z. Wang, "Group escape behavior of multiple mobile robot system by mimicking fish schools," in *2010 IEEE International Conference on Robotics and Biomimetics*, 2010, pp. 320–326.
- [44] R.-D. Cioarga, M. V. Micea, V. Cretu, and V. Groza, "Evaluation of fish shoal inspired movement in collaborative robotic environments," in *2010 IEEE Instrumentation & Measurement Technology Conference Proceedings*. IEEE, 2010, pp. 1539–1544.

- [45] S. Podila and Y. Zhu, "Animating multiple escape maneuvers for a school of fish." in *Graphics Interface*, 2017, pp. 140–147.
- [46] A. Jadbabaie, J. Lin, and A. S. Morse, "Coordination of groups of mobile autonomous agents using nearest neighbor rules," *IEEE Transactions on automatic control*, vol. 48, no. 6, pp. 988–1001, 2003.
- [47] A. E. Turgut, H. Çelikkanat, F. Gökçe, and E. Şahin, "Self-organized flocking in mobile robot swarms," *Swarm Intelligence*, vol. 2, no. 2-4, pp. 97–120, 2008.
- [48] F. Berlinger, J. Dusek, M. Gauci, and R. Nagpal, "Robust maneuverability of a miniature, low-cost underwater robot using multiple fin actuation," *IEEE Robotics and Automation Letters*, vol. 3, no. 1, pp. 140–147, 2017.
- [49] F. Gerlotto, S. Bertrand, N. Bez, and M. Gutierrez, "Waves of agitation inside anchovy schools observed with multibeam sonar: a way to transmit information in response to predation," *ICES Journal of Marine Science*, vol. 63, no. 8, pp. 1405–1417, 2006.
- [50] C. Agrillo, M. Dadda, G. Serena, and A. Bisazza, "Do fish count? spontaneous discrimination of quantity in female mosquitofish," *Animal cognition*, vol. 11, no. 3, pp. 495–503, 2008.